ISSN: 2521-5035 (Print)
ISSN: 2521-5043 (Online)

Contents List available at RAZI Publishing
Earth Science Malaysia (ESMY)
Journal Homepage: http://www.razipublishing.com/journals/earth-science-malaysia-esm/
https://doi.org/10.26480/esmy.01.2017.32.35

X-RAY DIFFERACTION ANALYSIS FOR THE INTERPRETATION OF CLAY MINERALS PARAGENESIS IN THE NEOGENE SEDIMENTS OF MANG AND VICINITY, SUB-HIMALAYAS, PAKISTAN

Muhammad Yasin*, Muhammad Ibrahim[1]

*Institute of Geology, University of Azad Jammu and Kashmir, Muzaffarabad, Pakistan
[1]Plant operator at Fauji Fertilizer Company Limited, Pakistan.
*Corresponding Author: Rajayasinkhan@gmail.com

ARTICLE DETAILS

Article history:

Received 24 October 2016
Accepted 7 December 2016
Available online 3 January 2017

Keywords:

Interpreted, Paragenesis, diffractometer, climes, epizonal.

ABSTRACT

The Neogene sediments were interpreted to understand the clay mineral paragenesis in rocks using x-ray differaction technique. The process was conducted with an x-ray diffractometer, Anode = Cu (Cu Kα = 1.541871 Å), Filter = Ni, Current = 15 mA and Voltage = 35 kv. The clay mineral assemblages in the rocks indicates that the neogene sediments were derived from the preexisting sedimentary, metasedimentary, metamorphics and igneous rocks and formed in different climes in the continental environment. The illite crystallinity (IC) value (0.2165 Δ°2θ CuKα) in the area correspond exactly with the epizonal metamorphic conditions.

1. Introduction

The X-ray differaction analysis of Neogene sediments was carried out in the Mang and adjoining areas at latitude 33° 45' 00" N to 33° 51' 30" N and Longitude 73° 35' 36" E to 73° 45' 00" E, the area being shown on toposheet No. 43/G-9, Survey of Pakistan (Yasin, 2014), in the Sub-Himalayan Foreland basin of Pakistan. The Murree and Nagri Formations among Neogene sediments were selected for X-ray differaction analysis.

Figure 1. The northwestern Himalayas of Pakistan displayed on the tectonic map (after Baig and Lawrence, 1987; Monalisa and Khawaja, 2004). The location of the project area being shown by a rectangle.

2. Previous work

The geology of the region was studied by different workers (Wadia, 1928; Ashraf and Chaudhary, 1984). However, the present work deals with the first comprehensive study of the area using X-ray differaction analysis.

3. Geological setting

The Himalayan orogen was formed about 55 Ma ago during Indo-Eurasian collision. About 30 to 40 Ma ago the rocks were metamorphosed during crustal thickening and about 20 Ma ago during granitic melting some movement along the South Tibet Detachment Zone has been observed (Garzanti et al., 2006). The continuous convergence propelled the thrust belt towards the south. During middle to late Miocene or early Pliocene times the Main Boundary Thrust (MBT) was active and thrusted the lesser Himalayan zone over Sub-Himalaya (Garzanti et al., 2006). At present times the Main Boundary Thrust (MBT) separates Lesser Himalayan zone above from the Tertiary Foreland Neogene sedimentary basin below. The material in the Foreland basin was deposited by means of distributary channels. Among these sediments the clays and shale are inundated stream (flood plain) deposits.

The mountains in the remote recesses as observed in the project area are known for their serene heights, arduous ascents and calmness in solitude (Yasin, 2014). They are also precipitous in places. The Jassa Pir peak with an altitude of over 216, 3 m has few sublime influences. Furthermore, the snowy scalps are pinnacled in mist and cloud and the area is very bleak in winter. However, the countryside is extremely parched by the sun during summer. The most alluring and captivating landscapes are also possessed by the area.

4. Methodology

In order to understand the paragenesis, eight rock samples of clays and shale (C-1, C-2, C-4, C-5, C-7,2014). The x-ray differaction analysis of the clays and shales was carried out in the Chemistry Department, Quaid-e-Aazam University, Islamabad, Pakistan. The results were further interpreted at the petrology Laboratory, University of Azad Jammu and Kashmir, Muzaffarabad, Pakistan. In x-ray differaction analysis the samples were first ground into fine powder, mounted on the slides before bombarding with the x-rays. The XRD analyses was conducted with an x-ray diffractometer, Anode = Cu (Cu Kα = 1.541871 Å), Filter = Ni, Current = 15 mA and Voltage = 35 kv. The X-ray differaction analysis commonly governed by the differaction of rays within the body of material revealed acute remarks on mineralogy and illite crystallinity. The diagnostic peaks on the chart differactogram are the illustrations of the relation of the intensity versus differaction angle on X and Y-axis respectively (Figs. 2 to 9).

5. Results and Discussions

5.1 X-Ray Differaction Analysis of Clays And Shales

The Neogene rock samples according to the geological classifications belong to the Murree and Nagri Formations.

The mineral assemblage in the rock samples of Murree rock Formation as identified through the differactogram includes illite, quartz, corrensite regular interstratified chlorite-montmorillonite, plagioclase feldspar-albite, smectite montmorillonite, muscovite, calcite, aragonite, siderite, kaolinite, dolomite, chlorite thuringite, gypsum, rectorite regular interstratified chlorite-montmorillonite, chlorite penninite, pyrite, goethite, alkali feldspar orthoclase, smectite saponite and lepidocrocite.

The mineral assemblage in the rock samples of Nagri rock Formation as identified through the differactogram includes illite, quartz, corrensite regular interstratified chlorite-montmorillonite, plagioclase feldspar-albite, calcite, aragonite, smectite saponite, siderite, pyrite, goethite, chlorite thuringite, haematite, smectite montmorrilonite lepidocrocite, rectorite-regular interstratified mica-montmorillonite, gypsum, plagioclase feldspar-albite, chlorite penninite, muscovite, haematite and dolomite.

The results have been enumerated under the tables 1 to 8 and plotted on the figures 2 to 9.

The illite crystallinity is measured in the rock samples (C-8 & C-2) collected from the northeastern and southwestern part of the study area (Yasin, 2014) respectively. The illite crystallinity (IC) value of 0.2165 Δ° 2θ CuKα (Fig. 10) in the area correspond exactly with the epizonal metamorphic conditions (Kubler, 1967, 68, 84). It can be elicited through the research that the (IC) value of 0.2165 Δ°2θ CuKα remained uniform in both of the formations exposed towards the northeastern and southwestern part of the study area (Fig. 10, Fig.11).

Table. 1: Showing the mineralogical composition of Nagri clays (Sample No. C-1).

Peak No.	Identified Minerals	Pos.[2th value calculated	Pos.[2th Original value	d-spacing Value calculated	d-spacing Original value	FWHM	Intensity %
1	Illite	19.8844	19.82	4.46519	4.48	0.2362	6.51
2	Quartz	20.9076	20.85	4.24892	4.26	0.0787	17.27
3	Corrensite	25.2109	25.23	3.53258	3.53	0.6298	2.07
4	Quartz	26.6767	26.67	3.34172	3.343	0.1181	100
5	Albite	27.9021	27.92	3.19768	3.196	0.2362	6.41
6	Calcite	29.4668	29.43	3.03134	3.035	0.0984	14.89
7	Aragonite	33.2192	33.18	2.69701	2.700	0.4723	2.69
8	Smectite Saponite	35.011	35.05	2.56298	2.56	0.3149	8.79
9	Quartz	36.5801	36.56	2.45656	2.458	0.1574	9.1
10	Quartz	39.503	39.49	2.28128	2.282	0.059	9.93
11	Siderite	42.5025	42.44	2.12697	2.13	0.1574	6.2
12	Aragonite	45.6601	45.90	1.98696	1.977	0.7872	2.48
13	Calcite	48.5902	48.55	1.87377	1.875	0.2362	3.52
14	Quartz	50.1589	50.21	1.81879	1.817	0.0787	10.13
15	Pyrite	55.3242	56.34	1.66059	1.633	0.9446	1.45
16	Quartz	59.9875	60.03	1.54089	1.541	0.072	6.2
17	Dolomite	68.2957	67.42	1.37227	1.389	0.384	5.48

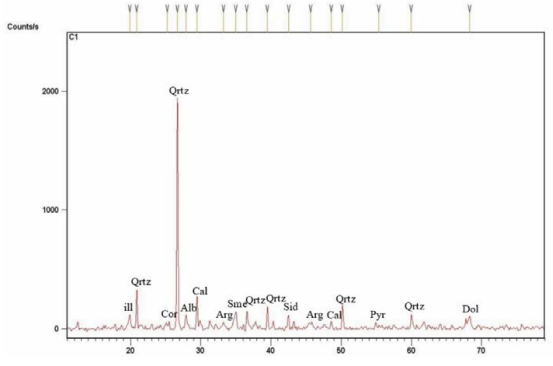

Fig. 2: Showing diffractogram of Nagri clays. ill = illite, Qrtz = Quartz, Cor = Corrensite, Alb = Albite, Cal = Calcite, Arg = Aragonite, Sme = Smectite, Sid = Siderite, Pyr = Pyrite.

Table. 2: Showing mineralogical composition of Nagri clays (Sample No. C-2).

Peak No.	Identified minerals	Pos.[2th Value calculated	Pos.[2th value obtained	d-spacing value calculated	d-spacing value obtained	FWHM	Intensity %
1	Corrensite	12.4333	12.50	7.1193	7.08	0.2362	2.39
2	Illite	19.9202	19.82	4.45725	4.48	0.2362	3.6
3	Quartz	20.9236	20.85	4.24572	4.26	0.1771	14.49
4	Goethite	21.3732	21.25	4.15741	4.18	0.3149	1.59
5	Chlorite Thuringite	25.1273	25.15	3.54414	3.541	0.9446	1.91
6	Illite	26.6924	26.77	3.33979	3.33	0.1968	100
7	Albite	27.9796	27.92	3.189	3.196	0.3149	3.4
8	Smectite Saponite	35.0534	35.05	2.55997	2.56	0.2165	5.92
9	Goethite	36.6106	36.65	2.45459	2.452	0.1771	7.15
10	Quartz	39.5187	39.49	2.28041	2.282	0.1968	5.98
11	Pyrite	40.3615	40.79	2.23471	2.212	0.2362	3.15
12	Siderite	42.5193	42.44	2.12617	2.13	0.1968	4.64
13	Aragonite	45.8418	45.90	1.9795	1.977	0.1574	3.86
14	Quartz	50.1926	50.21	1.81764	1.817	0.1968	8.5
15	Hematite	54.9573	54.28	1.6708	1.690	0.2362	2.89
16	Quartz	59.987	60.03	1.54218	1.541	0.1771	5.07
17	Smectite Montmorillonite	61.7781	61.85	1.5017	1.50	0.4723	1.95
18	Dolomite	68.3704	67.42	1.37209	1.389	0.2755	5.44
19	Dolomite	73.4153	67.42	1.2887	1.389	1.152	1.16

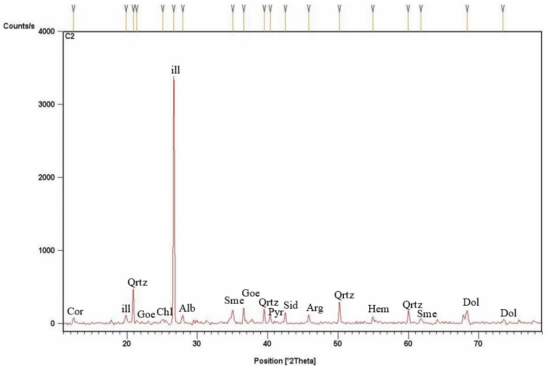

Fig. 3: Showing diffractogram of Nagri clays. Cor = Corrensite, ill = illite, Qrtz = Quartz, Goe = Goethite, Chl = Chlorite, Alb = Albite, Sme = Smectite, Pyr = Pyrite, Sid = Siderite, Arg = Aragonite, Hem = Hematite, Dol = Dolomite.

Table 3: Showing mineralogical composition of Murree shale (Sample No. C-4).

Peak No.	Identified Minerals	Pos.[2th Calculat-ed Values	Pos.[2th Standard values	d-spacing Calculated Values	d-spacing Standard values	FWHM	Intensity %
1	Illite	19.82	19.808	4.48	4.48386	0.2362	7.63
2	Quartz	20.85	20.894	4.26	4.25166	0.1181	16.98
3	Corrensite	25.23	25.3976	3.53	3.50703	0.4723	2.88
4	Quartz	26.67	26.6695	3.343	3.3426	0.1378	100
5	Plagioclase feldspar-Albite	27.92	27.911	3.196	3.19668	0.2362	4.75
6	Smectite Montmorillon-ite	29.58	29.4663	3.02	3.0314	0.1378	59.42
7	Muscovite	35.00	34.9909	2.564	2.5644	0.1968	11.65
8	Calcite	36.00	36.0826	2.495	2.48928	0.1574	9.64
9	Quartz	36.56	36.583	2.458	2.45637	0.1181	10.22
10	Aragonite	37.93	37.7091	2.372	2.38557	0.3149	4.89
11	Quartz	39.49	39.4873	2.282	2.28214	0.059	17.99
12	Siderite	42.44	42.4244	2.13	2.1307	0.4723	6.33
13	Calcite	43.18	43.237	2.095	2.09252	0.2362	9.64
14	Aragonite	45.90	45.6979	1.977	1.9854	0.7872	2.01

Table. 4: Showing mineralogical composition of Nagri clays (Sample No. C-5).

PeakNo.	Identified Minerals	Pos.[2th Calculated values	Pos.[2th Standard values	d-spacing Calculated values	d-spacing Standard values	FWHM	Intensity %
1	Illite	19.87	19.82	4.4684	4.48	0.3149	5.24
2	Quartz	20.908	20.85	4.24884	4.26	0.0787	16.87
3	Quartz	26.691	26.67	3.33995	3.343	0.1181	100
4	Lepidocrocite	27.8725	27.10	3.201	3.29	0.2362	4.99
5	Smectite Saponite	35.0344	35.05	2.56132	2.56	0.1181	9.73
6	Quartz	36.5771	36.56	2.45676	2.458	0.0787	9.73
7	Aragonite	37.7668	37.93	2.38206	2.372	0.4723	2.65
8	Quartz	39.5061	39.49	2.2811	2.282	0.059	7.23
9	Pyrite	40.3607	40.79	2.23476	2.212	0.1181	4.41
10	Siderite	42.5201	42.44	2.12613	2.13	0.1574	6.65
11	Aragonite	45.8686	45.90	1.97841	1.977	0.2362	3.99

12	Quartz	50.1751	50.21	1.81673	1.817	0.072	10.72
13	Quartz	50.3234	50.21	1.81622	1.817	0.072	5.65
14	Hematite	54.9046	54.28	1.67089	1.690	0.144	3.66
15	Quartz	59.993	60.03	1.54076	1.541	0.12	7.98
16	Smectite Montmorilloite	61.8195	61.85	1.49955	1.50	0.384	3.66
17	Hematite	64.1026	64.14	1.45154	1.452	0.576	2
18	Dolomite	68.3164	67.42	1.37191	1.389	0.384	5.82
19	Dolomite	75.7376	67.42	1.25485	1.389	0.288	2.49

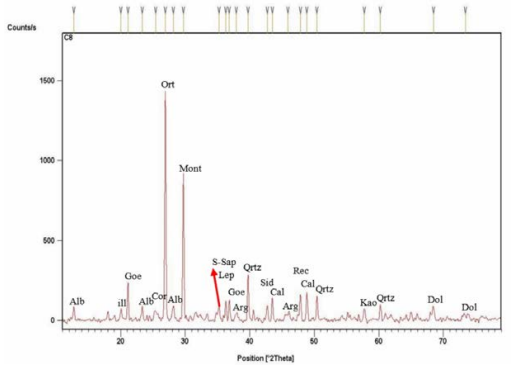

Fig. 7: Showing diffractogram of Murree clays. Alb = Albite, ill = illite, Goe = Goethite, Cor = Corrensite, Ort = Orthoclase, Mont. = Montmorillonite, S-Sap = Smectite Saponite, Lep = Lepidocrocite, Goe = Goethite, Arg = Aragonite, Sid = Siderite, Cal = Calcite, Rec = Rectorite, Qrtz = Quartz, Kao = Kaolinite, Dol = Dolomite.

Table. 7: Showing mineralogical composition of Nagri shale (Sample No. C-9).

Peak No.	Identified Minerals	Pos.[2th. Calculated values	Pos.[2th Standard values	d-spacing Calculated values	d-spacing Standard values	FWHM	Intensity %
1	Chlorite Thuringite	12.5269	12.52	7.06632		0.1968	8.8
2	Rectorite	17.8199	17.95	4.97757	4.94	0.2362	4.57
3	Corrensite	18.8076	18.80	4.71835	4.72	0.2362	3.46
4	Illite	19.8047	19.82	4.48299	4.48	0.4723	3.1
5	Gypsum	20.894	20.80	4.25167	4.27	0.1574	15.42
6	Gypsum	23.1331	23.47	3.84495	3.79	0.1968	5.1
7	Corrensite	25.2172	25.23	3.53172	3.53	0.1574	8.03
8	Quartz	26.6718	26.67	3.34232	3.343	0.1968	100
9	Albite	27.96	27.92	3.19119	3.196	0.1968	8.42
10	Calcite	29.4801	29.43	3.03001	3.035	0.2165	63.55
11	Chlorite Thuringite	31.6765	31.44	2.82475	2.845	0.9446	2.35
12	Chlorite Penninite	35.0268	35.05	2.56186	2.56	0.2362	6.06
13	Calcite	36.0687	36.00	2.49021	2.495	0.2165	8.35
14	Goethite	36.5929	36.65	2.45573	2.452	0.1771	8.58
15	Aragonite	37.766	37.93	2.38211	2.372	0.4723	2.01
16	Quartz	39.5015	39.49	2.28136	2.282	0.1968	16.18
17	Pyrite	40.3365	40.79	2.23604	2.212	0.2362	3.46
18	Siderite	42.4741	42.44	2.12832	2.13	0.1771	5.97
19	Calcite	43.2452	43.18	2.09215	2.095	0.1771	7.95
20	Muscovite	45.5651	45.37	1.99088	1.999	0.6298	4.27
21	Rectorite	47.6187	47.82	1.9097	1.902	0.2165	9.29
22	Calcite	48.6167	48.55	1.87281	1.875	0.2165	9.35
23	Quartz	50.1826	50.21	1.81798	1.817	0.2165	9.02
24	Hematite	55.1076	54.28	1.6666	1.690	0.4723	2.18
25	Pyrite	57.5234	56.34	1.60222	1.633	0.2362	4.21
26	Quartz	59.9885	60.03	1.54214	1.541	0.1574	6.18
27	Dolomite	68.3498	67.42	1.37133	1.389	0.336	5.11

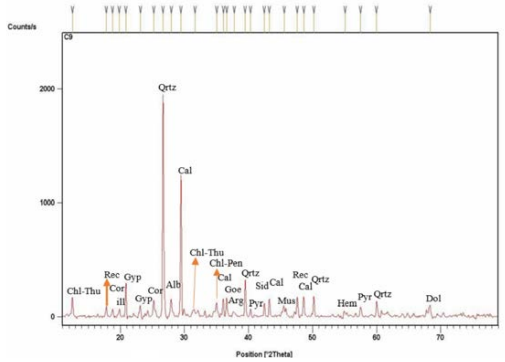

Fig. 8: Showing diffractogram of Nagri shale. Chl-Thu = Chlorite Thuringite, Rec = Rectorite, Cor = Corrensite, ill = illite, Gyp = Gypsum, Qrtz = Quartz, Cal = Calcite, Chl-Pen = Chlorite Penninite, Goe = Goethite, Arg = Aragonite, Pyr = Pyrite, Sid = Siderite, Mus = Muscovite, Hem = Haematite, Dol = Dolomite.

Table. 8: Showing mineralogical composition of Murree clays (Sample No. C-10).

Peak No.	Identified Minerals	Pos.[2th Calculated values	Pos.[2th Standard values	d-spacing Calculated values	d-spacing Standard values	FWHM	Intensity %
1	Illite	19.8367	19.82	4.47584	4.48	0.3149	7.55
2	Quartz	20.9116	20.85	4.24813	4.26	0.0787	13.5
3	Albite	23.1026	23.54	3.84996	3.78	0.2362	5.37
4	Illite	26.7048	26.77	3.33827	3.33	0.1181	100
5	Lepidocrocite	27.8016	27.10	3.20901	3.29	0.4723	3.05
6	Calcite	29.4719	29.43	3.03083	3.035	0.1181	45.28
7	Chlorite Penninite	35.0381	35.05	2.56105	2.56	0.551	11.76
8	Aragonite	36.0499	36.21	2.49147	2.481	0.2362	6.82
9	Quartz	36.5871	36.56	2.45611	2.458	0.1181	10.01
10	Quartz	39.5101	39.49	2.28088	2.282	0.1574	16.26
11	Siderite	42.504	42.44	2.1269	2.13	0.1181	7.55
12	Calcite	43.2841	43.18	2.09036	2.095	0.1968	10.6
13	Aragonite	45.7223	45.90	1.9844	1.977	0.7872	3.63
14	Calcite	47.5809	47.53	1.91113	1.913	0.1574	8.42
15	Calcite	48.5783	48.55	1.8742	1.875	0.2362	7.26
16	Quartz	50.1903	50.21	1.81772	1.817	0.1968	10.89
17	Quartz	59.9856	60.03	1.54221	1.541	0.1181	7.98
18	Smectite Montmorillonite	61.7508	61.85	1.50229	1.50	0.4723	5.52
19	Dolomite	68.2894	67.42	1.37352	1.389	0.2362	7.26
20	Dolomite	73.2977	67.42	1.29048	1.389	1.152	1.45

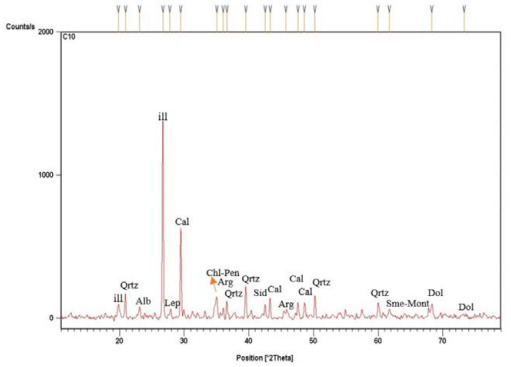

Fig. 9: Showing diffractogram of Murree clays. ill = illite, Qrtz = Quartz, Alb = Albite, Lep =Lepidocrocite, Cal = Calcite, Chl-Pen = Chlorite Penninite, Arg = Aragonite, Sid = Siderite, Sme-Mont = Smectite Montmorillonite, Dol = Dolomite.

5.2 Clay Mineralogy

The formation of illite in the Neogene sediments can be attributed to the decomposition of feldspar, deformation of muscovite and other diagenetic processes in a sedimentary environment (Deer et al., 1966). The alternate layers of two clay types (illite-smectite) are known as Rectorite (Hugget et al., 2001). The smectite in Neogene sediments is formed through neomorphism of soils and alteration of volcanic ash. The Corrensite (regular interstratified chlorite-montmorillonite) is sourced from the altered igneous rocks of basic composition and sandstone rock fragments (Hugget et al., 2001). The saponite exists in the mineral viens and basalt cavities (Deer et al., 1966). The basaltic rocks exposed in the area are Permian Panjal volcanics.

The albite and orthoclase are detrital in origin and are sourced from plutonic rocks and metamorphic rocks of green schist facies exposed in the Himalayan belt. The hematite, goethite and lepidochrocite indicate oxidizing conditions at the time of deposition of formation (Deer et al., 1966). The pyrite in the rock samples indicates that the reducing conditions exist in the part of basin. In Neogene sediments the calcite, aragonite, dolomite, pyrite, sulphur and quartz are found in association with gypsum. The limestone and dolomite are the fine grained detrital materials in the clays and shale. The coarse clasts of these rocks are present in sandstone (Yasin, 2014). The calcite, dolomite and gypsum in the rock could also exist through the pore water precipitation. The stratified rocks and hydrothermal minerals may act as the source material for siderite in the rock. The aragonite in the bulk composition is added from the agglutinated tests of organisms. The muscovite is sourced from regionally metamorphosed sediments, intermediate and acidic igneous rocks of the Himalayan mountains. Similarly, the chlorite is sourced from regionally metamorphosed sediments and hydrothermal alteration of pyroxene in mafic volcanic rocks (Deer et al., 1966). It is usually sourced from Al-rich hornblende in a reaction (Deer et al., 1966). The chlorites occur in metabasalts of Panjal volcanics. It also fills amygdules in Panjal volcanic rocks.

The clay minerals are detrital that retain their original character of source material, modified slightly in the depositional envireonment during diagenesis or neomorphism. The illite, montmorrilonite and illite-montmorrillonite are found in all depositional environments. Their alteration is common in fluviatile and subaerial environments. The chlorite forms authigenically in fresh water environment. The kaolinite is a dominant mineral in fluvial environment and hence own

continental origin (Grim et al., 1949). Illite and chlorite are usually formed at very cold, hot and dry climate.

Illites, irregularly mixed layers, vermiculites and smectites are formed at temperate climatic conditions. Similarly the kaolinites are formed in subarid as well as hot wet climates (Hugget et al., 2001). The illite also remains stable at moderate climatic conditions and remains unaltered during fluvial transport over short distance while the presence of kaolinite in clays and shales indicates that the acidic conditions may prevail, organic matter may be present in the environment of deposition.

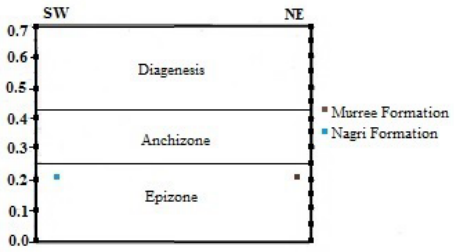

Fig. 10: Illite crystallinity (0.2165 Δ°2θ) in the Northeast and south west of the study area on a profile.

The Neogene sediments are deposited from the Mid Miocene to the Early Pleistocene (Chaudhri and Mahavir, 2012). The fold and thrust structures developed during tectonic activity increased the relief as well as erosion rate of hinterland (Chaudhri and Mahavir, 2012). As a result the sediments are deposited in the adjacent foredeep. The summer Monsoon is one of the significant factor that supplied sediments to the foreland basin (Saki et al., 2006).

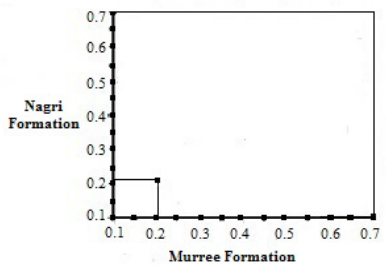

Fig. 11: The illite crystallinity value of the Nagri Formation and the Murree Formation coincides at (0.2165 Δ°2θ).

6. Conclusion

The study of Neogene sediments in the area indicates that the clay minerals were formed by the decompositions, deformations, alterations, neomorphism, pore water precipitations, authigenesis and other diagenetic processes at varied climes from Mid Miocene to the Early Pleistocene in the epizonal conditions and deposited by means of different stream patterns.

References

[1] Ashraf, M., Chaudhary, M. N., 1984. Petrology of lower Siwalik rocks of Poonch area: Kashmir Journal of Geology, 2: 1-10.

[2] Baig, M.S., Lawrence, R.D., 1987. Precambrian to early Paleozoic orogenesis in the Himalaya: Kashmir Journal of Geology, 5: 1-22.

[3] Chaudhri, A. R., Mahavir, S., (2012). Clay minerals as climate change indicators. American Journal of climate, 1:231-239.

[4] Deer, W. A., Howie, R. A., Zussman, J., (1966). An introduction to the rock-forming minerals. Longman group, London, 528 pp.

[5] Garzanti, E., Critelli, S., Ingersoll, R.V., (1996). Paleogeographic and paleotectonic evolution of the Himalayan Range as reflected by detrital modes of Tertiary sandstones and modern sands (Indus transects, India and Pakistan). Geological Society of America Bulletin, 108: 631–642.

[6] Grim, R. E., Dietz, R. S., Bradley, W. F., (1949). Clay mineral composition of some sediments from the Pacific Ocean off the California coast and the Gulf of California: Geological Society of America, Bulletin, 60: 1785-1808.

[7] Hugget. J. M., Gale, A. S., Clauer, N., (2001). The nature and origin of non-marine 10Å green Clays from the late Eocene and Oligocene of the Isle of Wight (Hampshire basin), UK. Clay Minerals, 36: 447-464.

[8] Kübler B. 1967. La cristallinité de l`illite et les zones tout a fait superieures du métamorphisme. In: Étages tectoniques, Colloque de Neuchâtel 1966, A La Baconniere, Neuchâtel, 105-121.

[9] Kübler B. 1968. Evaluation quantitative du métamorphisme par la cristallinité d l'illite. Bulletin, Centre Rech. Pau--S.N.P.A. 2: 385-397.

[10] Kübler, B., (1984). Les indicateurs des transformations physiques et chimiques dans la diagenèse, température et calorimétrie. in: "Thermobarométrie et barométrie géologiques", M. Lagache ed., Society of France Minéralogy and Cristallogrphy, Paris, 489-596.

[11] Monalisa and Khawaja, A.A., 2004. Structural trends and focal mechanism studies in the Potwar area with special emphasis on hydrocarbon exploration: Pakistan Journal of Hydrocarbon Research, 14: 49-59.

[12] Wadia, D. N., (1928). The geology of the Poonch State (Kashmir) and adjacent portion of the Punjab: Geological Survey of India, Memoirs, 51 (2): 185-370.

[13] Yasin, M., (2014). Petrography and Sedimentology of Neogene sediments in Mang and adjoining areas in the Sub Himalayas, Azad Jammu and Kashmir, Pakistan, Unpublished MS Thesis, University of Azad Jammu and Kashmir, Muzaffarabad, pp. 213.